

# Solitary waves in elongated clouds of strongly-interacting bosons

M. Ögren<sup>1</sup>, G. M. Kavoulakis<sup>1</sup>, and A. D. Jackson<sup>2</sup>

<sup>1</sup>*Mathematical Physics, Lund Institute of Technology, P.O. Box 118, SE-22100 Lund, Sweden*

<sup>2</sup>*Niels Bohr Institute, Blegdamsvej 17, DK-2100, Copenhagen Ø, Denmark*

(Dated: May 1, 2019)

We examine the propagation of solitary waves in elongated clouds of trapped bosonic atoms as the confinement, the strength of the interatomic interaction, and the atom density are varied. We identify three different physical regimes and develop a general formalism that allows us to interpolate between them. Finally we pay special attention to the transition to the Tonks-Girardeau limit of strongly-interacting bosons.

PACS numbers: 05.45.Yv,05.30.Jp,67.40.Db

By appropriate manipulation of the trapping potential, confined ultracold atoms can achieve conditions of reduced dimensionality. Taking advantage of this property, two recent experiments described in Refs. [1, 2] have managed to create conditions such that bosonic atoms approached the so-called Tonks-Girardeau phase [3] predicted for strongly-interacting bosons in one dimension. In the experiment of Ref. [2], bosonic atoms were confined in elongated traps, and the gas was observed to approach the Tonks-Girardeau limit as the transverse confinement was increased. Evidence for this transition was obtained from measurements of the energy and of the axial size of the gas. In the experiment of Ref. [1] the momentum distribution provided evidence for this transition.

Motivated by these experiments, we will consider here how solitary waves emerge in strongly-interacting, quasi-one-dimensional atomic gases. We first present a general description of the problem, identifying three physically distinct regimes [4]. We then develop a formalism that allows us to calculate the density profile, energy, and momentum associated with grey/dark solitary waves [5, 6, 7, 8, 9, 10, 11, 12]. This formalism can be applied to any quasi-one dimensional system given only knowledge of the energy per unit length as function of the density per unit length. We find interesting changes in the properties of solitary waves as a function of density which suggest that the study of solitary waves in these elongated clouds could provide confirmation of the transition to the Tonks-Girardeau limit [13, 14]. Our results also suggest eventual technological applications, e.g., the transmission of signals in atomic waveguides.

Here, we will neglect the effects of trapping along the  $z$ -axis of weak confinement and will for simplicity consider a cylindrical trap,  $V = M\omega_{\perp}^2(x^2 + y^2)/2$ , where  $M$  is the atom mass, and  $\omega_{\perp}$  is the frequency of the trapping potential in the transverse direction. We approximate a short-ranged atom-atom interaction as  $V_{\text{int}}(\mathbf{r} - \mathbf{r}') = U_0\delta(\mathbf{r} - \mathbf{r}')$  where  $U_0 = 4\pi\hbar^2 a/M$  and  $a$  is the s-wave scattering length for elastic atom collisions. The Gross-Pitaevskii equation for the order parameter,  $\Psi$ , then has

the form

$$i\hbar\partial_t\Psi = (-\hbar^2\nabla^2/2M + U_0|\Psi|^2 + V)\Psi. \quad (1)$$

Following Ref. [15], we assume that the transverse dimension of the cloud is sufficiently small and the corresponding time scale sufficiently short that the transverse profile of the particle density can adjust to the equilibrium form appropriate for the local atomic density. With this approximation, the problem becomes one-dimensional, and the solitary pulse can be described by a local velocity,  $v(z)$ , and a local density of particles per unit length,  $\sigma(z) = \int |\Psi(x, y, z)|^2 dx dy$  [15]. The order parameter can then be written as a simple product [7] with  $\Psi(\mathbf{r}, t) = f(z, t)g(x, y, \sigma)$ , where  $g$  is the equilibrium wavefunction for the transverse profile. If  $g$  is chosen to be normalized,  $\int |g|^2 dx dy = 1$ , the equations above imply that  $|f|^2 = \sigma$ .

In this problem there are three qualitatively distinct physical regimes and two corresponding transitions separating them. The first of these transitions involves a change in the transverse profile of the cloud. For weak transverse confinement,  $|g|^2$  can be calculated using the Thomas-Fermi approximation and is simply a parabola. For transverse confinement of a strength sufficient to ensure that the chemical potential is much smaller than  $\hbar\omega_{\perp}$ ,  $|g|^2$  becomes Gaussian. The second transition involves a change in the longitudinal profile of solitary waves. For weak transverse confinement, the atoms form a condensate. In the limit of strong interactions, strong transverse confinement and small linear densities, however, bosonic atoms behave in a certain sense like non-interacting fermions. This transition involves no change in the (Gaussian) transverse profile since the chemical potential of the gas is much smaller than  $\hbar\omega_{\perp}$  in both cases.

We first consider the transition in the transverse direction. The critical value of  $\sigma a$  for this transition is determined by the condition that the kinetic energy associated with transverse motion,  $\hbar^2/MR^2$ , is comparable to the typical interaction energy,  $nU_0$ , where  $R$  is the transverse width of the cloud and  $n$  is the typical (three-dimensional) density. Since  $n \sim N/(Z\pi R^2)$ ,

where  $N/Z = \sigma$  is the density per unit length, one sees that the value of  $\sigma$  at the crossover is  $\sigma_{c,1} \sim 1/a$ . It is interesting to note that both energy scales vary as  $1/R^2$  with the consequence that  $\sigma_{c,1}$  is independent of the oscillator length  $a_{\perp} = (\hbar/M\omega_{\perp})^{1/2}$ .

Under typical experimental conditions (i.e., where a single trap rather than a series of tubes is used),  $\sigma a \gg 1$ . The cloud is thus in the Thomas-Fermi regime. The situation changes, however, with greater transverse confinement. To see this, we recall that the cloud expands along the long axis of the trap when it is squeezed transversely. Since  $Z$  increases,  $\sigma = N/Z$  decreases.

In the limit  $\sigma a \ll 1$ ,  $|g|^2$  has a Gaussian form,  $|g|^2 = e^{-(\rho/a_{\perp})^2}/(\pi a_{\perp}^2)$ . As shown in Ref. [7],  $f$  then satisfies the equation

$$i\hbar \partial_t f = -(\hbar^2/2M)\partial_z^2 f + \hbar\omega_{\perp}(1 + 2a|f|^2)f. \quad (2)$$

We see from this equation that  $f \propto e^{-i\omega_{\perp}(1+2a\sigma_0)t}$  as  $|z| \rightarrow \infty$ , where  $\sigma_0$  is the background linear density. Rewriting Eq. (2) using the variable  $w = fe^{i\omega_{\perp}(1+2a\sigma_0)t}$ , we obtain

$$i\hbar \partial_t w = -(\hbar^2/2M)\partial_z^2 w + \hbar\omega_{\perp}2a(|w|^2 - \sigma_0)w. \quad (3)$$

Equation (3) includes a familiar (i.e., quadratic) nonlinear term and leads to a speed of sound,  $c_1$ , which satisfies the equation  $Mc_1^2 = 2\hbar\omega_{\perp}\sigma_0 a$ . Since  $\sigma_0 = n_0\pi a_{\perp}^2$ , we see that  $Mc_1^2 = n_0U_0/2$  [7].

As shown in Refs. [7, 11], the density associated with a solitary wave of velocity  $u$  has the form

$$\sigma(z)/\sigma_0 - 1 = -\cos^2\theta/\cosh^2(z \cos\theta/\zeta), \quad (4)$$

where  $\theta = \sin^{-1}(u/c_1)$  and  $\zeta = 2\xi(n_0)$ . Here  $\xi(n_0)$  is the coherence length for  $n_0 = \sigma_0/(\pi a_{\perp}^2)$ , so that  $\zeta = a_{\perp}/(2\sigma_0 a)^{1/2}$ . Further, the dispersion relation connecting the energy and momentum of a solitary wave,  $\mathcal{E}(\mathcal{P})$ , is given parametrically as  $\mathcal{E}/\mathcal{E}_0 = (4\sqrt{2}/3)\cos^3\theta$ , where  $\mathcal{E}_0 = \hbar\omega_{\perp}(\sigma_0 a)^{1/2}\sigma_0 a_{\perp}$ , and  $\mathcal{P}/\mathcal{P}_0 = \pi u/|u| - 2\theta - \sin 2\theta$ , where  $\mathcal{P}_0 = \sigma_0\hbar$ .

We now consider the second, longitudinal transition. As noted above, the gas approaches the so-called Tonks-Girardeau limit, in which the bosons to some extent behave like non-interacting fermions, as the transverse confinement is increased. The motion of the atoms in this limit is effectively one-dimensional since transverse degrees of freedom are frozen out when  $\hbar\omega_{\perp}$  is much larger than the chemical potential. In the crossover region, each atom occupies a length of order  $1/\sigma_0$  along the axis of the trap. The corresponding kinetic energy is on the order of  $\hbar^2\sigma_0^2/M$ . The typical interaction energy, on the other hand, is on the order of  $n_0U_0$ , where  $n_0 \sim \sigma_0/a_{\perp}^2$  so that  $n_0U_0 \sim \hbar^2\sigma_0 a/(Ma_{\perp}^2)$ . Thus, the ratio between the interaction energy and the kinetic energy is  $\sim a/(\sigma_0 a_{\perp}^2) \sim [\sigma_0\xi(n_0)]^{-2}$ . Given the assumption of strong interactions, this quantity is much larger than

unity for small values of  $\sigma_0$  (i.e., for low densities), small values of  $a_{\perp}$  (i.e., for strong transverse confinement), or large values of  $a$  (i.e., for strong interactions). The transition between the two regimes takes place for  $\sigma_{c,2} \sim a/a_{\perp}^2$ .

For values of  $\sigma_0$  much smaller than  $\sigma_{c,2}$  [16],

$$i\hbar \partial_t f = (\hbar^2/2M)(-\partial_z^2 f + \pi^2|f|^4 f). \quad (5)$$

In this case we see that  $f \propto e^{-i(\pi^2\sigma_0^2\hbar/2M)t}$  as  $|z| \rightarrow \infty$ . We thus rewrite Eq. (5) using the variable  $w = fe^{i(\pi^2\sigma_0^2\hbar/2M)t}$  to obtain

$$i\hbar \partial_t w = (\hbar^2/2M)[-\partial_z^2 w + \pi^2(|w|^4 - \sigma_0^2)w]. \quad (6)$$

The speed of sound  $c_2$  is now given as  $Mc_2^2 = \pi^2\hbar^2\sigma_0^2/M$  or  $c_2 = \pi\hbar\sigma_0/M$ . This is precisely the Fermi velocity in one dimension with  $k_F = \sigma_0\pi$ .

As shown in Ref. [8], the density of the cloud associated with the solitary wave is now

$$\sigma(z)/\sigma_0 - 1 = -\frac{3\cos^2\theta}{2 + (1 + 3\sin^2\theta)^{1/2} \cosh(2\pi\sigma_0 z \cos\theta)}, \quad (7)$$

where  $\theta = \sin^{-1}(u/c_2)$ . The dispersion relation can again be expressed parametrically using

$$\mathcal{E}/\mathcal{E}_0 = \frac{\sqrt{3}\pi}{2} \cos^2\theta \ln \left[ \frac{2 + 3\cos^2\theta}{(1 + 3\sin^2\theta)^{1/2}} \right], \quad (8)$$

with  $\mathcal{E}_0 = \hbar^2\sigma_0^2/M$ , and

$$\mathcal{P}/\mathcal{P}_0 = -\pi(\mathcal{E}/\mathcal{E}_0) \tan\theta + \cos^{-1} \left[ \frac{3\sin^2\theta - 1}{(1 + 3\sin^2\theta)^{1/2}} \right]. \quad (9)$$

It is natural to ask how one actually proceeds from one region to another. The transverse transition was studied in some detail in Refs. [7, 12]. Here, we focus on the second, longitudinal transition using a formalism of more general applicability. The basic ingredient required is the equation of state, i.e., the energy of the gas per unit length,  $\epsilon(\sigma)$ , as function of  $\sigma$ . This can be calculated from the Lieb-Liniger model [17] and can be written as  $\epsilon(\sigma) = (\hbar^2\sigma^3/2M)\tilde{\epsilon}(\gamma)$ , where  $\tilde{\epsilon}(\gamma)$  is a numerically known function and  $\gamma = 2a/(\sigma a_{\perp}^2)$ .

Given  $\epsilon(\sigma)$ , one can immediately determine the sound velocity as  $Mc^2 = \sigma_0\partial^2\epsilon/\partial\sigma^2(\sigma_0)$ . The energy of the solitary wave is

$$\mathcal{E} = \int \left( \frac{\hbar^2}{2M} \frac{\partial w^*}{\partial z} \frac{\partial w}{\partial z} + \epsilon(\sigma) - \sigma\epsilon'(\sigma_0) + C \right) dz \quad (10)$$

with  $\epsilon' = \partial\epsilon/\partial\sigma$ . The final term in this equation represents the energy of the background density of atoms and ensures convergence of the integral. Thus,  $C = -\epsilon(\sigma_0) + \sigma_0\epsilon'(\sigma_0)$ .

Equation (10) implies that  $w$  satisfies the equation

$$i\hbar \partial_t w = -(\hbar^2/2M)\partial_z^2 w + [\epsilon'(\sigma) - \epsilon'(\sigma_0)]w. \quad (11)$$

Writing  $w = \sqrt{\sigma} e^{i\phi}$  and separating the real and imaginary parts of Eq. (11), we obtain the two hydrodynamic equations

$$\frac{\hbar^2}{2M} \left( \frac{\partial \sqrt{\sigma}}{\partial z} \right)^2 = \epsilon(\sigma) - \epsilon(\sigma_0) - (\sigma - \sigma_0) \epsilon'(\sigma_0) - Mu^2 \frac{(\sigma - \sigma_0)^2}{2\sigma} \quad (12)$$

and  $v = (\hbar/M) \partial \phi / \partial z = u(1 - \sigma_0/\sigma)$ . Here, we have imposed the boundary condition that  $v \rightarrow 0$  as  $\sigma \rightarrow \sigma_0$ . Eq. (10) can be written as

$$\mathcal{E} = \int \left[ \frac{\hbar^2}{2M} \left( \frac{\partial \sqrt{\sigma}}{\partial z} \right)^2 + \frac{\hbar^2 \sigma}{2M} \left( \frac{\partial \phi}{\partial z} \right)^2 + \epsilon(\sigma) - \epsilon(\sigma_0) - (\sigma - \sigma_0) \epsilon'(\sigma_0) \right] dz. \quad (13)$$

Combining the above equations, we obtain

$$\mathcal{E} = 2 \int [\epsilon(\sigma) - \epsilon(\sigma_0) - (\sigma - \sigma_0) \epsilon'(\sigma_0)] dz. \quad (14)$$

Finally, the momentum of the solitary wave is given as

$$\mathcal{P} = M \int (\sigma - \sigma_0) v(z) dz = Mu \int \frac{(\sigma - \sigma_0)^2}{\sigma} dz. \quad (15)$$

We thus see that, given knowledge of the energy per unit length  $\epsilon(\sigma)$ , Eq.(12) allows us to determine the shape of the solitary wave  $\sigma(z)$  for a given velocity,  $u$ . Equations (14) and (15) then give  $\mathcal{E}(u)$  and  $\mathcal{P}(u)$ , which can be combined to establish the dispersion relation,  $\mathcal{E} = \mathcal{E}(\mathcal{P})$ . While the profiles of the solitary wave and the corresponding dispersion relations are known in all three limits examined earlier [5, 6, 8, 10, 11, 12], Eqs. (11) – (15) allow us to interpolate between them. As indicated, our approach is quite general and merely requires knowledge of  $\epsilon(\sigma)$ .

Let us now consider a specific example for the case  $\gamma_0 = 2a/(\sigma_0 a_\perp^2) = 1$ . It is convenient to express  $\epsilon$  explicitly in terms of  $\sigma$  with the result that  $\epsilon(\sigma) = [\hbar^2 \sigma_0^3 / 2M] \tilde{\epsilon}(\sigma/\sigma_0)$ , where a reliable interpolation formula for  $\tilde{\epsilon}$  is given as  $\tilde{\epsilon}(y) = (\pi^2 \gamma_0^3 y^3 / 3 + \kappa \gamma_0 y^5) / (\gamma_0^3 + 4\gamma_0^2 y + 4\gamma_0 y^2 + \kappa y^3)$  with  $y = \sigma(z)/\sigma_0$  and  $\kappa \approx 6.879$ .

For  $\gamma_0 = 1$ , Eq. (12) then has the form

$$\left( \frac{\partial \sqrt{y}}{\partial \tilde{z}} \right)^2 = \frac{\pi^2 y^3 / 3 + \kappa y^5}{1 + 4y + 4y^2 + \kappa y^3} - \frac{\pi^2 / 3 + \kappa}{9 + \kappa} - (y - 1) \frac{\partial \tilde{\epsilon} / \partial y|_{y=1}}{c^2} - \left( \frac{Mc}{\hbar \sigma_0} \right)^2 \frac{u^2 (y - 1)^2}{y}, \quad (16)$$

where  $\tilde{z} = \sigma_0 z$ . Given that  $\partial \tilde{\epsilon}(y) / \partial y \approx 1.471$  and  $\partial^2 \tilde{\epsilon}(y) / \partial y^2 \approx 1.872$  for  $y = 1$ , we find that the sound velocity is given as  $(Mc/\hbar \sigma_0)^2 \approx 0.936$ . For a given value of  $u/c$ , Eq. (16) gives the profile of the solitary wave  $\sigma(z)/\sigma_0$ . Figure 1 shows such solutions for  $u/c = 0.1$  (bottom curve at  $z = 0$ ), 0.4, 0.7, and 0.9 (top).

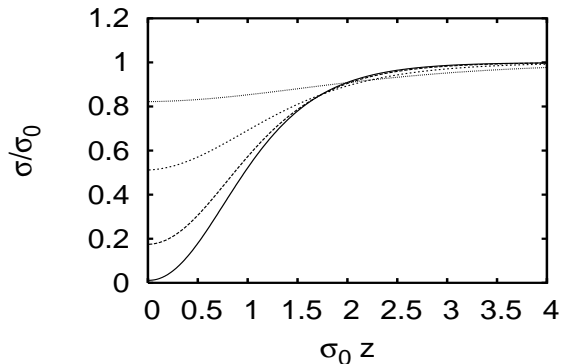


FIG. 1: The density  $\sigma(\tilde{z})/\sigma_0$  associated with a solitary wave given by the solution of Eq. (16), for  $\gamma_0 = 2a/(\sigma_0 a_\perp^2) = 1$  and  $u/c = 0.1$  (lowest graph at  $z = 0$ ), 0.4, 0.7, and 0.9 (highest), where  $\tilde{z} = \sigma_0 z$ .

The energy and the momentum can then be calculated from Eqs. (14) and (15):

$$\mathcal{E}(u) = \frac{\hbar^2 \sigma_0^2}{M} \int_{-\infty}^{+\infty} \left[ \frac{\pi^2 y^3 / 3 + \kappa y^5}{1 + 4y + 4y^2 + \kappa y^3} - \frac{\pi^2 / 3 + \kappa}{9 + \kappa} - 1.471 (y - 1) \right] d\tilde{z}, \quad (17)$$

and

$$\mathcal{P}(u) = Mu \int_{-\infty}^{\infty} d\tilde{z} (y - 1)^2 / y. \quad (18)$$

The dispersion relation  $\mathcal{E} = \mathcal{E}(\mathcal{P})$ , initially obtained by Lieb, is shown as the continuous (lower) line in Fig. 2. The maximum value of  $\mathcal{P}$  corresponds to a dark solitary wave with  $u = 0$ . For long wavelengths, the solitary waves become ordinary sound waves with the usual linear dispersion relation [6, 10, 11, 12]. From Eq. (11) one can also calculate the dispersion relation appropriate for the Bogoliubov mode. This has the usual form

$$\mathcal{E} = \sqrt{(\mathcal{P}^2 / 2M)^2 + (c\mathcal{P})^2}. \quad (19)$$

The Bogoliubov dispersion relation,  $\mathcal{E} = \mathcal{E}(\mathcal{P})$ , is shown as the dashed (higher) line in Fig. 2.

The two conditions derived above establishing the typical values of  $\sigma$  that characterize the three regimes,  $\sigma_{c,1} a \sim 1$  and  $\sigma_{c,2} a_\perp^2 \sim a$ , give values of  $\sigma$  which differ by roughly one order of magnitude when the transverse confinement is strong as in Ref. [2]. For example, for  $a \sim 100 \text{ \AA}$  and  $\omega_\perp = 2\pi \times 70.7 \text{ kHz}$  (which implies that  $a_\perp \sim 0.04 \text{ \mu m}$ ), we see that  $\sigma_{c,1} \sim 10^6 / \text{cm}$  and  $\sigma_{c,2} \sim 10^5 / \text{cm}$ .

Another remarkable feature of this problem is that it is independent of the scattering length in the Tonks-Girardeau limit. Specifically, in the two limiting cases (i.e., the one-dimensional Gross-Pitaevskii equation and the Tonks-Girardeau equation), the characteristic widths

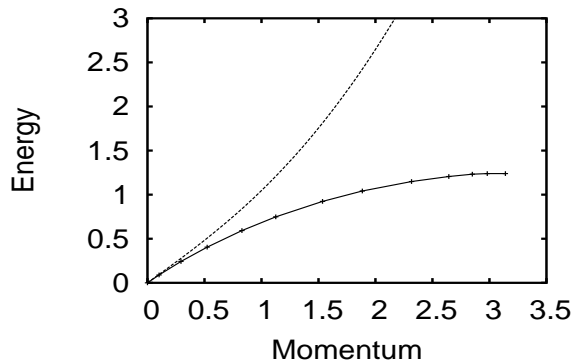


FIG. 2: The dispersion relation  $\mathcal{E} = \mathcal{E}(\mathcal{P})$  for solitary waves (lower) and for the Bogoliubov mode (higher). The momentum is measured in units of  $\hbar\sigma_0$ , and the energy is measured in units of  $\hbar^2\sigma_0^2/M$ . Here  $\gamma_0 = 2a/(\sigma_0 a_\perp^2) = 1$ .

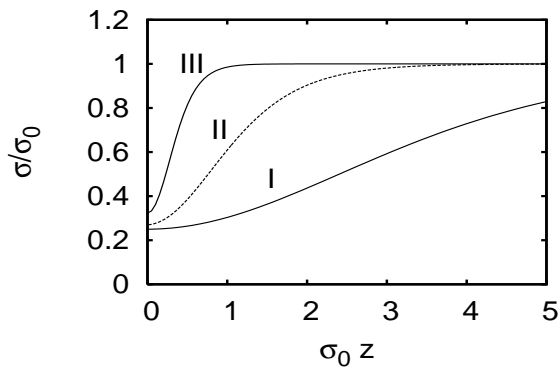


FIG. 3: The profile of the solitary waves for  $u/c = 1/2$  and three values of  $\gamma_0 = 2a/(\sigma_0 a_\perp^2)$ . In the lowest one (I)  $\gamma_0 = 1/10$ , corresponding to the one-dimensional Gross-Pitaevskii limit, Eq. (4), in the middle one (II)  $\gamma_0 = 1$ , corresponding to the intermediate regime, Eq. (16), and in the highest one (III)  $\gamma_0 = 10$ , corresponding to the Tonks-Girardeau limit, Eq. (7).

of solitary waves is on the order of the coherence length  $\xi \sim a_\perp/(\sigma_0 a)^{1/2}$  and on the order of the interparticle spacing  $1/\sigma_0$ , respectively. This allows us to understand the qualitative features of the profiles shown in Fig. 3. For the largest value of  $\sigma_0 = 10\sigma_c$ , which explores the Gross-Pitaevskii limit, the characteristic width of the disturbance (in units of  $\sigma_0^{-1}$ ) is on the order of  $(\sigma_0 a_\perp^2/a)^{1/2} \sim 1/\sqrt{\gamma_0}$ , which is larger than unity. In the opposite Tonks-Girardeau limit with  $\sigma = \sigma_c/10$ , the width is of order unity in units of  $\sigma_0^{-1}$ . Therefore, as one moves from one regime to the other, the width of the solitary wave in the dimensionless units of Fig. 3 decreases and eventually reaches a constant value of order unity. This fact can be used as an experimental signature of the transition from one limit to the other.

The present model is valid provided that the solitary

waves have a width which is larger than the atom-atom spacing. While our predictions are thus expected to be reliable for waves whose size is larger than  $1/\sigma_0$  (e.g., sound waves), they are pushed to the limits of their validity in the extreme cases of the Tonks-Girardeau limit ( $\gamma \gg 1$ ) and for narrow (and thus slow) pulses. Predictions in these regions are expected to be qualitatively, but not quantitatively, correct [8]. The Bogoliubov spectrum, on the other hand, agrees with the exact result [5] for  $\mathcal{P} \rightarrow 0$  and  $\mathcal{P} \rightarrow \infty$  for all values of  $\gamma$ .

Finally, as seen in Fig. 2, the dispersion relations for the two modes converge in the limit of long wavelength since both correspond to small amplitude sound waves in this limit. For shorter wavelengths, however, they diverge. The characteristic momentum,  $\mathcal{P}_c$ , for which differences appear is on the order of  $\hbar/\xi$ . Thus,  $\mathcal{P}_c/\mathcal{P}_0 \sim \sqrt{a/(\sigma_0 a_\perp^2)} \sim \sqrt{\gamma_0}$ , which is on the order of unity at the transition and larger than unity as one approaches the Tonks-Girardeau regime. This behavior is quite different from that between the three-dimensional and the one-dimensional problems studied in Refs. [10, 11, 12], where the two modes have different energies and momenta. In this respect the present problem more closely resembles the homogeneous problem initially studied by Lieb [5, 6].

We thank Nikos Papanicolaou and Stephanie Reimann for useful discussions. M.Ö. thanks Peter Drummond for presenting the Lieb-Liniger model to him. We also acknowledge financial support from the European Community project ULTRA-1D (NMP4-CT-2003-505457).

- 
- [1] B. Paredes *et al.*, Nature (London) **429**, 277 (2004).
  - [2] T. Kinoshita *et al.*, Science **305**, 1125 (2004).
  - [3] L. Tonks, Phys. Rev. **50**, 955 (1936); M. Girardeau, J. Math. Phys. (N.Y.) **1**, 516 (1960).
  - [4] E. H. Lieb *et al.*, Phys. Rev. Lett. **91**, 150401, 2003.
  - [5] E. H. Lieb, Phys. Rev. **130**, 1616 (1963).
  - [6] T. Tsuzuki, J. Low Temp. Phys. **4**, 441 (1971).
  - [7] A. D. Jackson *et al.*, Phys. Rev. A **58**, 2417 (1998).
  - [8] E. B. Kolomeisky *et al.*, Phys. Rev. Lett. **85**, 1146 (2000).
  - [9] M. D. Girardeau and E. M. Wright, Phys. Rev. Lett. **84**, 5691 (2000).
  - [10] S. Komineas and N. Papanicolaou, Phys. Rev. Lett. **89**, 070402 (2002).
  - [11] A. D. Jackson and G. M. Kavoulakis, Phys. Rev. Lett. **89**, 070403 (2002).
  - [12] S. Komineas and N. Papanicolaou, Phys. Rev. A **67**, 023615 (2003).
  - [13] S. Burger *et al.*, Phys. Rev. Lett. **83**, 5198 (1999).
  - [14] J. Denschlag *et al.*, Science **287**, 97 (2000).
  - [15] G. M. Kavoulakis and C. J. Pethick, Phys. Rev. A **58**, 1563 (1998).
  - [16] E. B. Kolomeisky and J. P. Straley, Phys. Rev. B **46**, 11749 (1992).
  - [17] E. H. Lieb and W. Liniger, Phys. Rev. **130**, 1605 (1963).